

Broadband Antennas Based on the Double Moebius Strip

Vadym Slyusar¹ , Ihor Sliusar² , Sergey Sheleg³ 

¹Central Research Institute of Armaments and Military Equipment of Armed Forces of Ukraine, Kyiv, Ukraine, swadim@ukr.net

²Department of Information Systems and Technologies Poltava State Agrarian Academy, Poltava, Ukraine, islyusar2007@ukr.net

³ENIT, Inc., Scottsdale, AZ, U.S.A., ssheleg@yahoo.com

Abstract— The family of new antenna designs based on the double Moebius strip principle is proposed in this article. Three possible options of the power supply port location had been reviewed in this respect: the cut external strip with the signal port located directly in the cut area is used; the continuous rings without discontinuities are applied, with the signal port located in the gap between the strips; the power supply port is located in the interstrip area, and there is a cut in one of the strips. The radio technical parameters of the antennas were researched by means of their modelling in Ansys HFSS packet. The strip width, its thickness, the interstrip gap, as well as the radius of the cylinder within which the antenna may be enabled, were used as mechanical parameters of the antennas based on the double Moebius strip. The best results were represented by the super-broadband antennas with the port located between two strips. In particular, 2-inch (50.8 mm) frequency independent antenna based on the singular continuous Moebius ring has a bandwidth of 38.648 GHz (from 11 to 49.648 GHz), and the frequency ratio (correlation of maximum operation frequency to the minimum one) exceeds 4.5. The application of the cut in the strip helped to improve the frequency response characteristics of such antenna, having increased its frequency ratio to the value of 5.548. In fact, the synthesized antennas occupy the intermediate niche between the double strip ring and the fractal antennas in terms of their characteristics. It makes it possible to use them in integrated communication, radio location, radio monitoring and navigation, both as independent structural units and as parts of wheeled gear structures of the crewless platforms.

Index Terms— Moebius strip, power supply, Ansys HFSS, Return Loss, VSWR.

I. INTRODUCTION

The important trend in terms of the development of the motor vehicle antennas is the decrease of dimensions and the extension of bandwidth of the antenna systems, which is conditioned by the increase of the number of various telecommunication standards which need support during the functioning process. Moreover, this miniaturization of the onboard devices is promoted by the trend of the integration of the communication systems implying the telecommunication issues solving [1]–[4]. A case in point is the application of the motor vehicle radars, operating in the millimeter wave range along with the application of cellular transmission 5G [5], [6].

As indicated in [7], the increase of interest to the application of the ring structures within the

development of the antenna systems has become the consequence of the above-mentioned trends. It is conditioned by the fact that unlike square, rhombus or triangle, they potentially enable larger amplification (the wider area is covered by the antenna element, the higher the amplification factor is). The bandwidth of the ring structures is several times broader than that of the common dipole. Besides, the ring structures can be more naturally integrated into the wheel construction of the automotive carriage frame [8]. In this respect, the works [7]–[10] represent the synthesis of the series of the ring antennas based on the application of single or double strips of smooth or quasi-fractal forms. One of the main tasks connected with their improvement, along with the optimization of adjustment, is the extension of the bandwidth. The application of the Moebius strip has been chosen as the potential way to obtain this, considering that the geometrical features of antenna within its fixed diameter can enable the extension of the operation bandwidth. The condenser execution in a form of a double Moebius strip ring, described in the USA mechanical patent [11], can be used as a basic point for the structural synthesis of specific antennas. The ideas of the application of the resonators in a form of the Moebius strip for the synthesis of the elementary cells of metamaterials represent the perspective viability of the electrodynamics of such structural concepts [12], [13].

The purpose of the article is the research of the dependency of the frequency response characteristics of the antennas based on the double Moebius strip on their geometrical parameters.

II. THE THEORETICAL ASPECTS OF THE DESCRIPTION OF THE MOEBIUS

There exist different options of the analytical description of the Moebius strip, varying by the method of representation (parametrically, as an equation with two unknown quantities and so on), reference system, choice of the reference point as well as the direction of the bypass of the supporting circle, definition of its radius etc. The most widely used one is the parametrical method of representation. Particularly, in [14] the corresponding option is considered with regard to the case with the supporting circle with the singular radius:

$$\begin{cases} x = \left(1 + \frac{t}{2} \cos\left(\frac{\nu}{2}\right)\right) \cos \nu \\ y = \left(1 + \frac{t}{2} \cos\left(\frac{\nu}{2}\right)\right) \sin \nu, \\ z = \frac{t}{2} \sin\left(\frac{\nu}{2}\right) \end{cases} \quad (1)$$

where $0 < \nu \leq 2\pi$, $-1 < t < 1$.

In [15, 16] two alternative options are represented, focused on the supporting circle of radius 2, defined by the expression $x^2 + y^2 = 4$. In the first of two ones, the reference point is the angle $u = 0$ [15, 16]:

$$\begin{cases} x = \left(2 - v \sin\left(\frac{u}{2}\right) \right) \sin u \\ y = \left(2 - v \sin\left(\frac{u}{2}\right) \right) \cos u . \\ z = v \cos\left(\frac{u}{2}\right) \end{cases} \quad (2)$$

It should be noted that in all the cases the factors outside trigonometric functions $\sin u$ and $\cos u$ within axes x and y are identical, and they are responsible for the representation of the rotation of the basic strip around the supporting circle.

In case the reference point coincides with the x -axis, then $u = \pi/2$, and the indicated system of the parametrical equations can be transformed by means of the substitution of u -angle by its modified version $\underline{u} = u + \pi/2$ [15]:

$$\begin{cases} x = \left(2 - v \sin\left(\frac{\pi}{4} + \frac{u}{2}\right) \right) \cos u \\ y = - \left(2 - v \sin\left(\frac{\pi}{4} + \frac{u}{2}\right) \right) \sin u . \\ z = v \cos\left(\frac{\pi}{4} + \frac{u}{2}\right) \end{cases} \quad (3)$$

The analysis of the indicated expressions enables their generalization in case of the arbitrary radius of the supporting circle R in this case the equation system (1) can be represented as follows:

$$\begin{cases} x = \left(R + \frac{tR}{2} \cos\left(\frac{v}{2}\right) \right) \cos v \\ y = \left(R + \frac{tR}{2} \cos\left(\frac{v}{2}\right) \right) \sin v . \\ z = \frac{tR}{2} \sin\left(\frac{v}{2}\right) \end{cases} \quad (4)$$

The same expression for the arbitrary radius of the supporting circle a is represented in [17]:

$$\begin{cases} x = \left(a + v \cos\left(\frac{u}{2}\right) \right) \cos u \\ y = \left(a + v \cos\left(\frac{u}{2}\right) \right) \sin u . \\ z = v \sin\left(\frac{u}{2}\right) \end{cases} \quad (5)$$

In case when the surface possesses certain thickness d , limited by two simultaneously rotating Moebius strips with radiuses R_1 and $R_2 = R_1 - d$, we will receive result as follows, based (4):

$$\begin{cases} x_1 = \left(R_1 + \frac{tR_1}{2} \cos\left(\frac{v}{2}\right) \right) \cos v \\ x_2 = \left(R_2 + \frac{tR_2}{2} \cos\left(\frac{v}{2}\right) \right) \cos v \\ y_1 = \left(R_1 + \frac{tR_1}{2} \cos\left(\frac{v}{2}\right) \right) \sin v \\ y_2 = \left(R_2 + \frac{tR_2}{2} \cos\left(\frac{v}{2}\right) \right) \sin v \\ z_1 = \frac{tR_1}{2} \sin\left(\frac{v}{2}\right) \\ z_2 = \frac{tR_2}{2} \sin\left(\frac{v}{2}\right) \end{cases} \quad (6)$$

The prototype of the antenna systems reviewed hereinafter is represented by the combination of two simultaneously rotating Moebius strips, both with the same thickness d , located as far from each other as the interval h . In fact, in terms of the considered parametrical representation it means four strips with the radiuses of the supporting circles R_1 and $R_2 = R_1 - d$, $R_3 = R_1 - d - h$ and $R_4 = R_1 - 2d - h$. As a result, the equation system (6) can be represented as follows:

$$\begin{cases} x_n = \left(R_n + \frac{tR_n}{2} \cos\left(\frac{v}{2}\right) \right) \cos v \\ y_n = \left(R_n + \frac{tR_n}{2} \cos\left(\frac{v}{2}\right) \right) \sin v, \\ z_n = \frac{tR_n}{2} \sin\left(\frac{v}{2}\right) \end{cases} \quad (7)$$

where $n = 1, 2, 3, 4$.

The correlations indicated above correspond with the single revolution of the supporting circle. For the arbitrary integer number of revolutions k the expression (7) is modified as follows:

$$\begin{cases} x_n = \left(R_n + \frac{tR_n}{2} \cos\left(k \frac{v}{2}\right) \right) \cos v \\ y_n = \left(R_n + \frac{tR_n}{2} \cos\left(k \frac{v}{2}\right) \right) \sin v, \\ z_n = \frac{tR_n}{2} \sin\left(k \frac{v}{2}\right) \end{cases} \quad (8)$$

where $n = 1, 2, 3, 4$.

As an example, two-band Moebius strip can be modelled in Mathcad [18] dataset in accordance with the following expressions:

$$\begin{cases} x_n = \left(R_n + \frac{tR_n}{Q} \cos\left(k \frac{v}{2}\right) \right) \cos(v + \beta) \\ y_n = \left(R_n + \frac{tR_n}{Q} \cos\left(k \frac{v}{2}\right) \right) \sin(v + \beta), \\ z_n = \frac{tR_n}{Q} \sin\left(k \frac{v}{2}\right) \end{cases} \quad (9)$$

where $n = 1, 2$; $R_1 = 5\pi = 15.708$; $R_2 = R_1 - 3$, $Q = 3$, $-0.5 \leq t \leq 0.5$, $0 \leq v \leq 2\pi$, $k = 3, 4, 5, 6, \dots$ – the number of revolutions of each of the strips, defining the variant of the polygon formed within the internal region of the strip, β is the angle providing the required orientation of the basement of this polygon towards the axes x and y .

This model describes two independent and simultaneously rotating Moebius strips. The values Q and W can be different integer numbers. The options of two-band ring corresponding with the expression (9) at different values of parameters k and β are represented in Fig. 1.

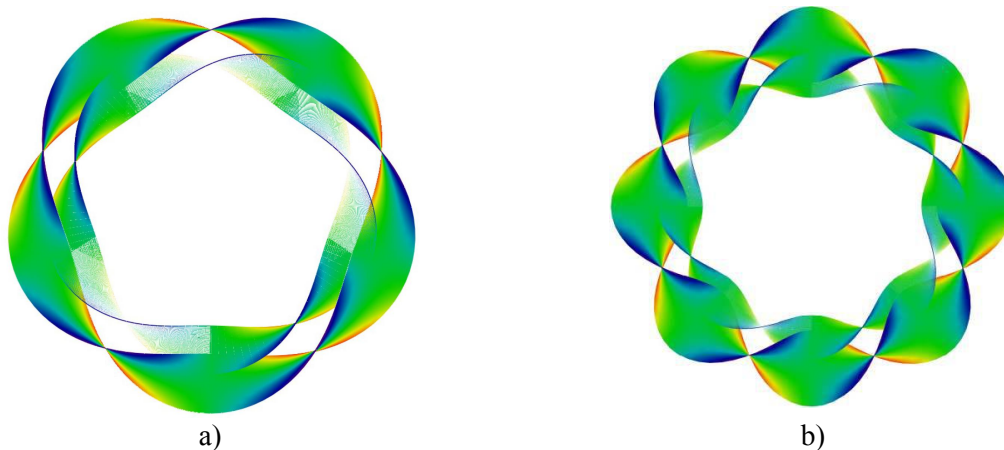


Fig. 1. The options of two-band Moebius ring at $k = 5$, $\beta = 13\pi/64$ (position a) and $k = 8$, $\beta = 0$.

Another variant of the representation is possible where two bands differ only in terms of the description of z -coordinate, for example:

$$\begin{cases} x_1 = \left(R_1 + \frac{tR_1}{Q} \cos\left(k \frac{v}{2}\right) \right) \cos v, \\ x_2 = x_1, \\ y_1 = \left(R_1 + \frac{tR_1}{Q} \cos\left(k \frac{v}{2}\right) \right) \sin v, \\ y_2 = y_1, \\ z_1 = \frac{tR_1}{Q} \sin\left(k \frac{v}{2}\right) \\ z_2 = z_1 + 4 \end{cases} \quad (10)$$

In this case two identical bands are shifted towards z -axis.

The reviewed options of analytical representations of two-band Moebius ring can be applied as a basis when synthesizing antenna designs in Ansys EM Suite system. Nevertheless, the expressions

(6) – (10) are not so useful independently in this process, because the design of Moebius strip in Ansys EM Suite is a non-trivial art. Moreover, the authors had obtained the alternative – in comparison with (6) – (10) variant of two-band ring during the process of this synthesis; where the pair of independent bands are integrated with each other forming the integral continuous surface. Considering the secondariness of the task for the analytical representation of the geometry of such design towards the antenna synthesis, its review is out of scope of the present article.

III. ANTENNAS BASED ON CONTINUOUS MOEBIUS STRIP

We will consider three potential options of the power supply port location within the active ring antenna:

the application of the cut external ring with the cut made in one of the strips, at that the signal port is located directly in the cut area of the strip;

the application of the continuous ring, without any discontinuities, and the signal port is located in the gap between strips;

the location of the signal port in the interstrip area along with the cut made in one of the strips. The conventional radio technical parameters had been used for the research of the characteristics of mentioned antennas types, namely: “Return Loss” and VSWR. Herewith, the width of the bandwidth of the antenna was defined in terms of the frequency range, within which the return loss does not exceed 10 dB, or VSWR amounts to value less than 2.0.

The frequency ratio, implying the correlation of maximum operation frequency to the minimum one, can be applied for the definition of the level of the antenna bandwidth, as well as such parameter as fractional bandwidth [19]:

$$\delta F = \frac{2|f_1 - f_2|}{f_1 + f_2}, \quad (11)$$

where f_1 and f_2 are the nominal values of minimum and maximum frequencies within which the values of VSWR or RL exceed the target level.

The examples of some of the antenna structures having been researched at the first stage are represented in Fig. 2.

The strip width, its thickness, the interstrip gap, as well as the radius of the cylinder within which the antenna may be enabled, were used as mechanical parameters of the antennas based on the continuous (without any discontinuities) double Moebius strip (Fig. 3).

The numeric values of corresponding parameters for the structures illustrated in Fig. 2 are represented in Table 1. Herein, the external diameter of the antenna equals approximately one inch (25.4 mm).

The most interesting ones from among the overall options illustrated in Fig. 2 are the structures with pentangular front view of the aerial area in the center, possessing the expressed symmetry (positions b and c in Fig. 2). Such structural option is formed as a result of strictly defined choice of

its parameters, among which the three-time correlation between the strip width and the interstrip gap is the key one. Moreover, the strip thickness, which being increased will cause the extension of the bandwidth of antenna, plays the significant role. At that the best choice is the option when the strip thickness equals to the interstrip gap.

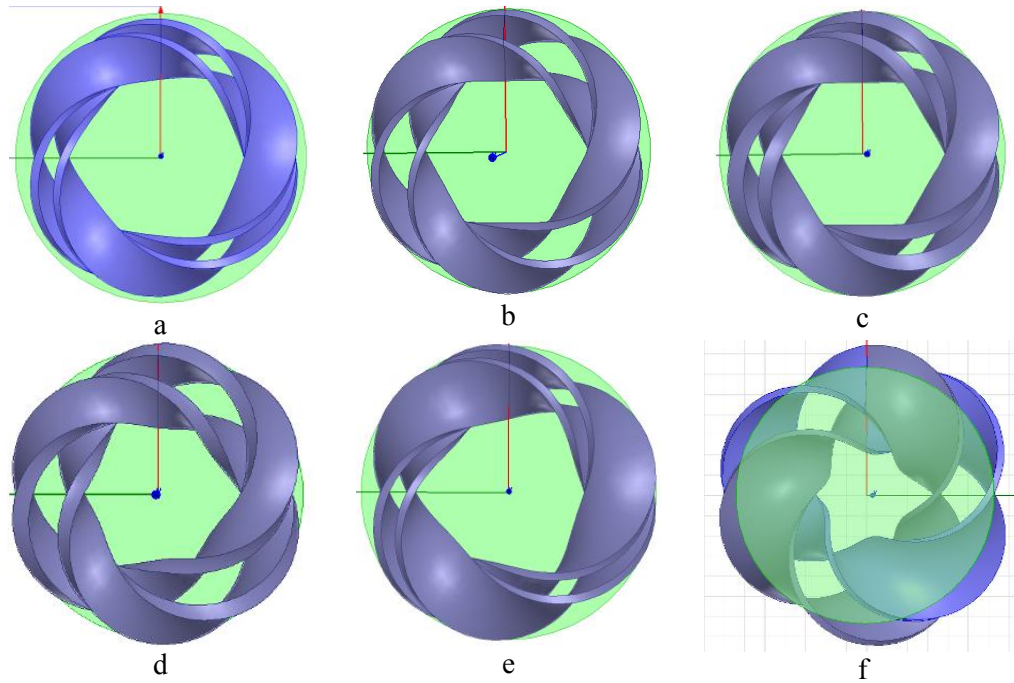


Fig. 2. The researched antenna options based on the double Moebius strip.

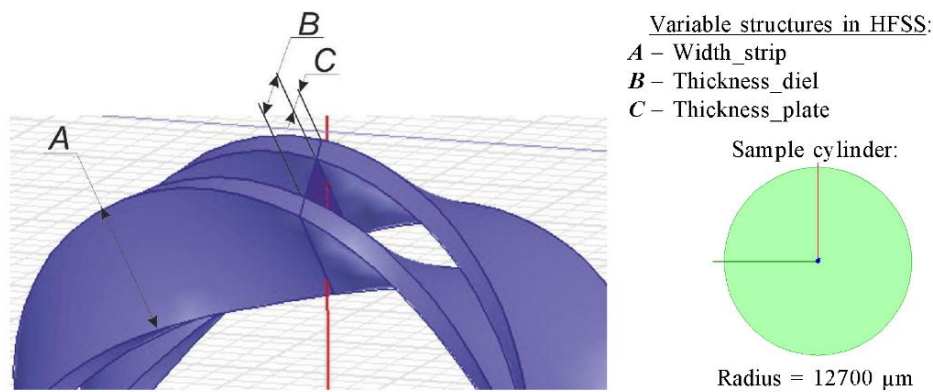


Fig. 3. The researched antenna options based on the double Moebius strip.

TABLE I. SIZES OF ANTENNA STRUCTURES

No.	View	Dimensions, μm		
		A	B	C
1	a	4500	1500	750
2	b	4500	3000	750
3	c	4500	1500	1500
4	d.	4500	3000	1500
5	e	6000	1500	750
6	f	9000	3000	750

For the purpose of the formation of the adequate antenna models as well as the possibility of the analysis of their features, the solution region (named Air Box) with the dimensions $74.295 \times 74.295 \times 74.295$ mm is set in the far field of Ansys EM Suite 2021 R1. It significantly exceeds the software requirements for the minimum values of the Air Box with regard to the dimensions of the proposed antennas. Such approach enables the application of the obtained research results in subsequent works where the specified geometry of antennas will be considered as the comparison standard. For example, two or more antenna can be set in this box.

The frequency dependencies of the return loss and VSWR of the antenna, of the corresponding position “c” in Fig. 2, are represented in Fig. 4, 5. The obtained results had proved the hypothesis about the efficiency of the antenna based on double Moebius strip in the broad band operation.

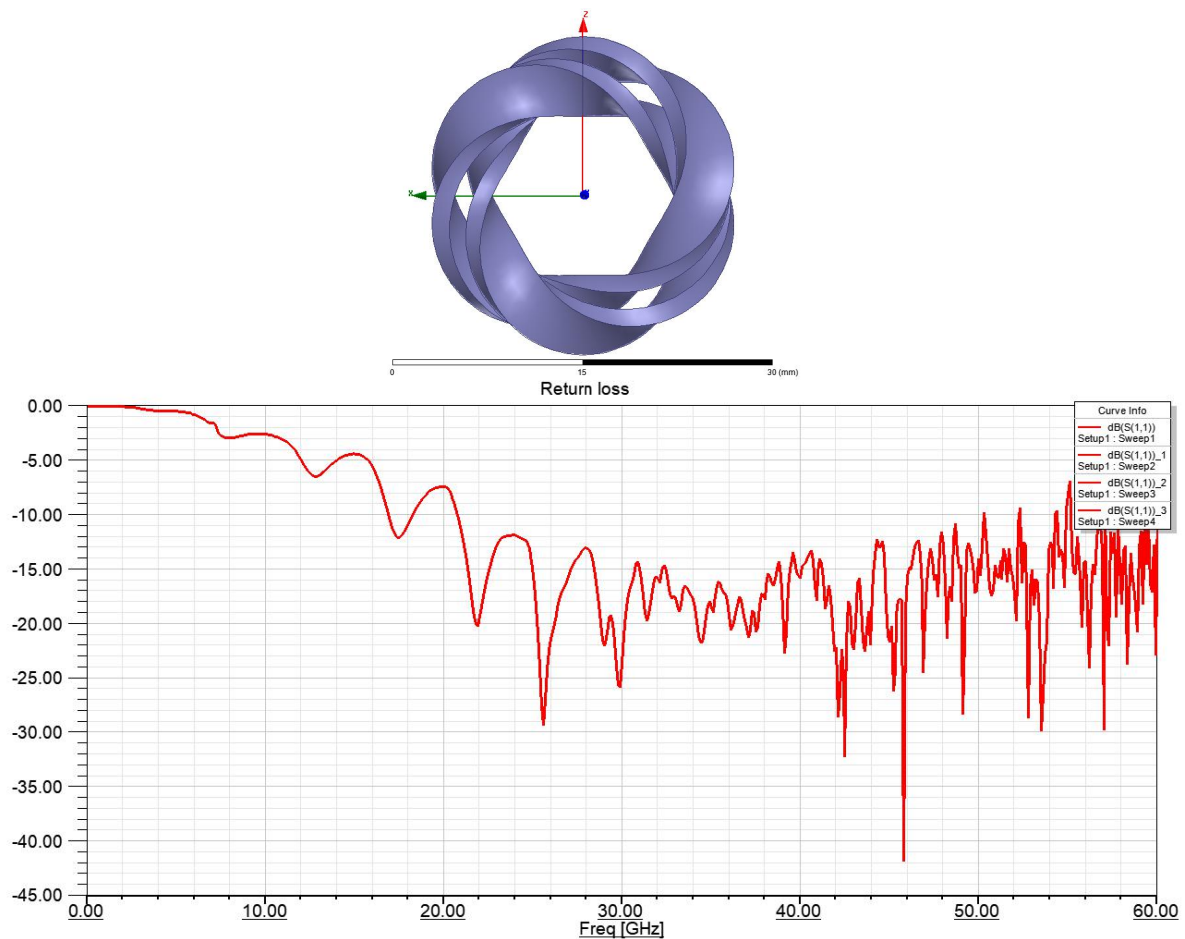


Fig. 4. The dependency of return loss on frequency.

The further research task has become the verification of scaling possibility of the received parameters of the structure enabled by antenna, into the lower frequency domain. For this purpose, all geometrical parameters had been doubled and the following values had been obtained: $A = 9000 \mu\text{m}$, $B = 3000 \mu\text{m}$, $C = 3000 \mu\text{m}$.

As expected, along with the increase of the external diameter of the ring the working frequency range shifts down in terms of the frequency level, shrinks in terms of its ultimate bandwidth and frequency ratio. The configuration of the designed antenna with the external diameter of 2 inches

(50.8 mm) is represented in Fig. 6. Based on the return loss and VSWR diagrams illustrated in Fig. 7, 8, the lower limit of the working area had shifted to 10.5 GHz, and the upper one moved to the level of 35.5 GHz. Also, the overall bandwidth of the antenna is 25 GHz, and the frequency ratio is approximately 3.38.

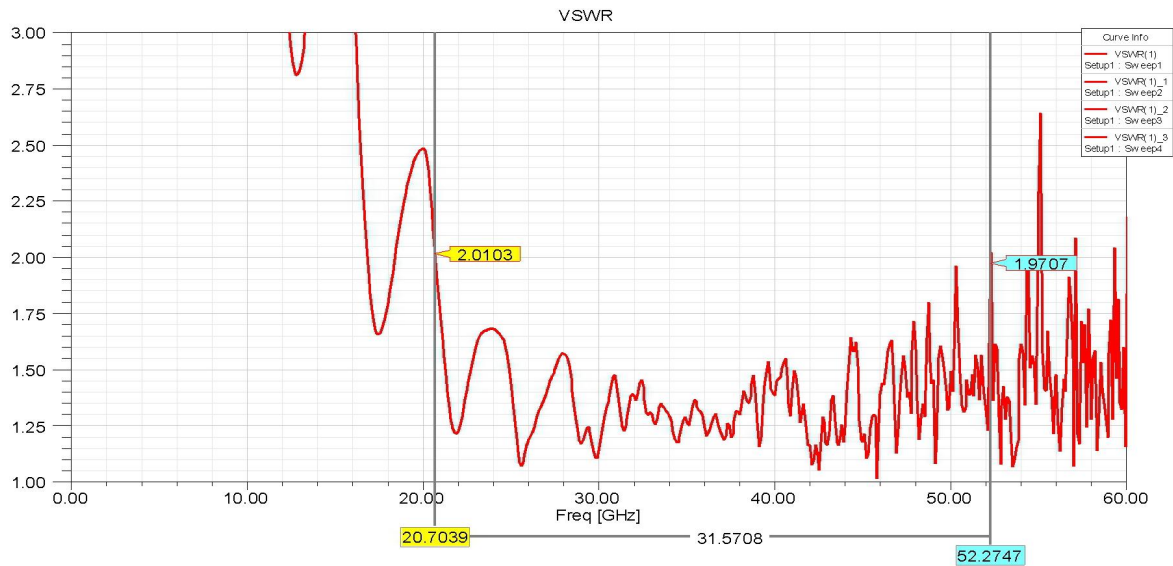


Fig. 5. The dependency of VSWR on frequency.

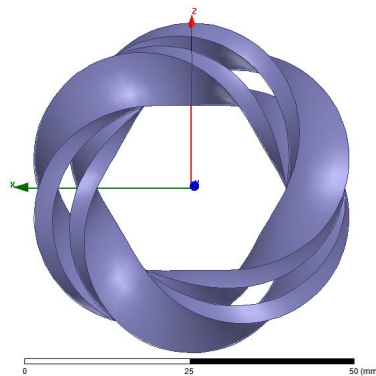


Fig. 6. The designed antenna with the external diameter of 2 inches (50.8 mm).

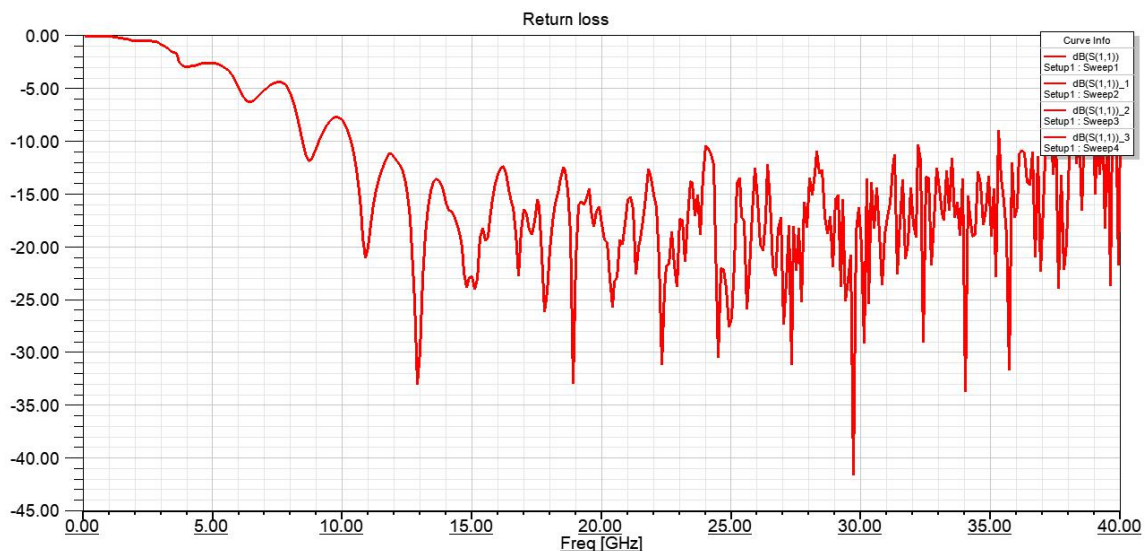


Fig. 7. The dependency of return loss on 2-inch (50.8 mm) antenna frequency.

The further variability of the parameters of the reviewed antenna allowed to receive the structures providing similar electrodynamic values by double decrease of the external diameter.

The first one is characterized by the additional spin of the strip when forming the Moebius surface. At that, the parameters $A=9000\ \mu\text{m}$, $B=3000\ \mu\text{m}$, $C=3000\ \mu\text{m}$ are used with the external diameter of antenna amounting 1 inch (25.4 mm). As a result, the construction was received, which is illustrated in Fig. 9 and possessing the internal aerial area with the front section view in a form of the hexagram star of David.

The characteristics of such antenna are represented in Fig. 10, 11. As we see, the operation bandwidth corresponding to the level of return loss less than 10 dB amounts 32 GHz (from 14 to 46 GHz). In case we disregard the outliers not exceeding 1 dB and which can be eliminated by more proper alignment of antenna and feeder, then the mentioned bandwidth extends up to 37 GHz (from 14 to 51 GHz). Looking back, the bandwidth with $VSWR \leq 2$ indeed corresponds with the frequency range of the return loss – 9.542 dB.

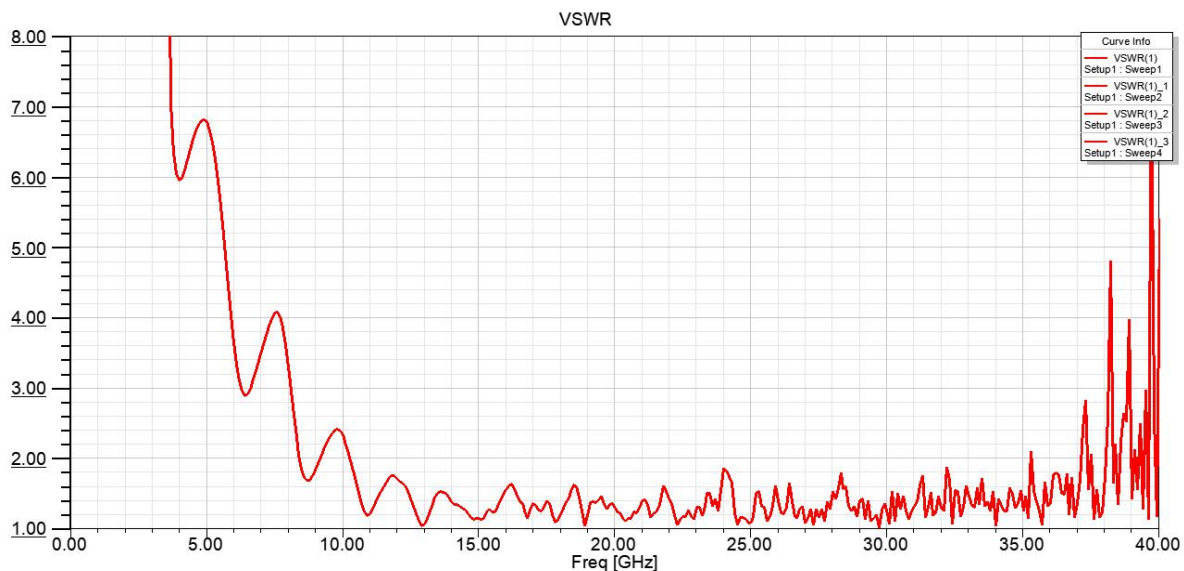


Fig. 8. The dependency of VSWR on 2-inch (50.8 mm) antenna frequency.

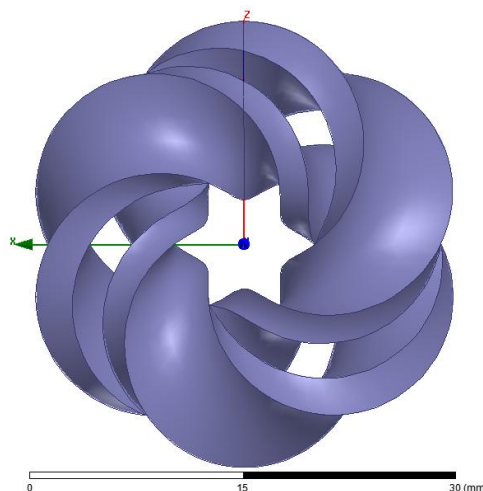


Fig. 9. Broadband antenna based on the ring in a form of the star of David.

The alternative variant of the antenna, named as a “singular” Moebius ring by the authors, due to its limit values of the geometrical parameters enabling the formation of this pattern, is represented in Fig. 12. The matter is that during the further increase of A, B, C values characterizing the topology of the antenna, the edges of the strip begin to adjoin. Moreover, this structure implies only one spin of the strip unlike at least 3 and 5 spins of the antennas in Fig. 2.c and 8 correspondingly.

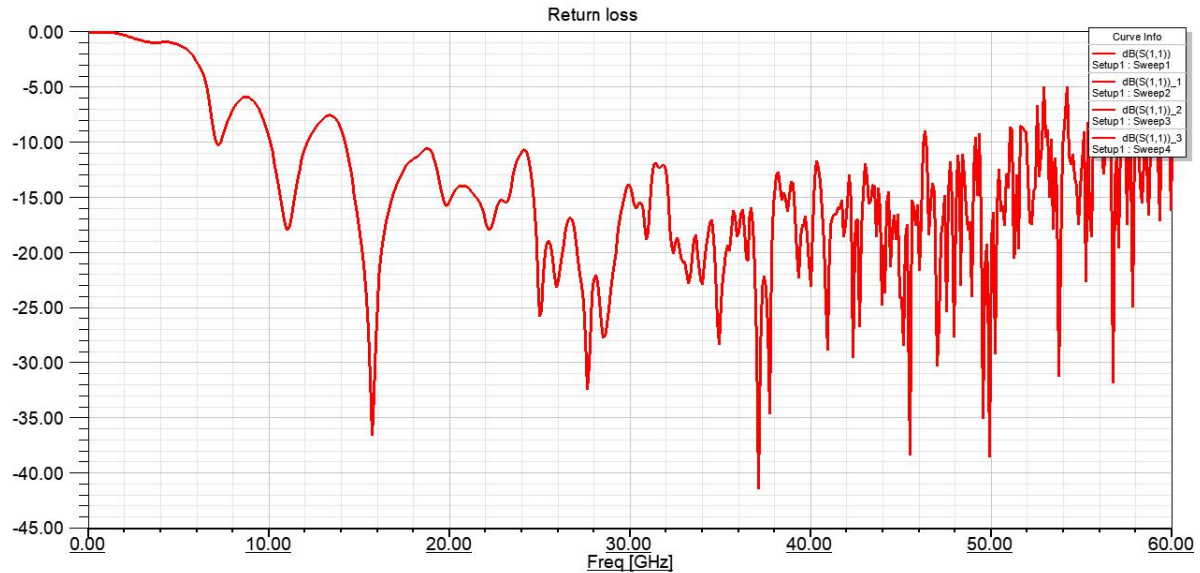


Fig. 10. The return loss of the antenna with the area shaped as the star of David.

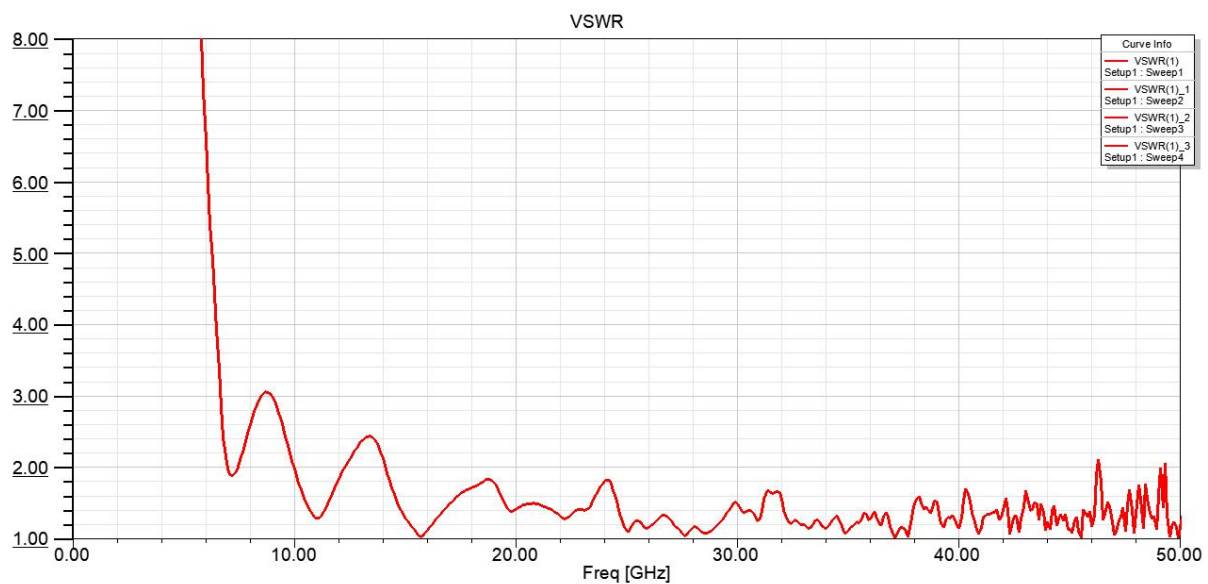


Fig. 11. VSWR of the antenna represented in Fig. 9.

Pursuant to Fig. 13, 14, illustrating the results of the research of the frequency dependencies of the return loss and VSWR values in Ansys HSFF packet, the bandwidth of “singular” antenna in case of $A = 9000$, $B = C = 3000$ μm amounts approximately 38.648 GHz (at the level of the return loss being 10 dB) and extends from 11 GHz to 49.648 GHz. At that the frequency ratio exceeds 4.5. Thus, the present structure of the frequency independent antenna based on the “singular” Moebius ring appears to be the most broadband from among all the researched ones and like the antenna reviewed in Fig. 9,

it surpasses the super-broadband antennas with the port located between two strips and possessing pentagonal shape view in the central area, in terms of parameters.

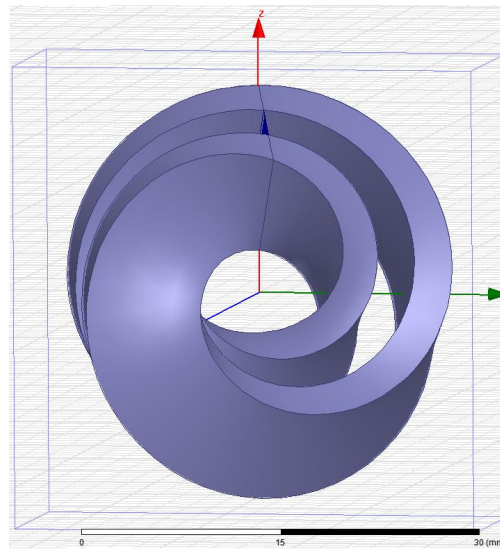


Fig. 12. The frequency independent antenna based on the “singular” Moebius ring.

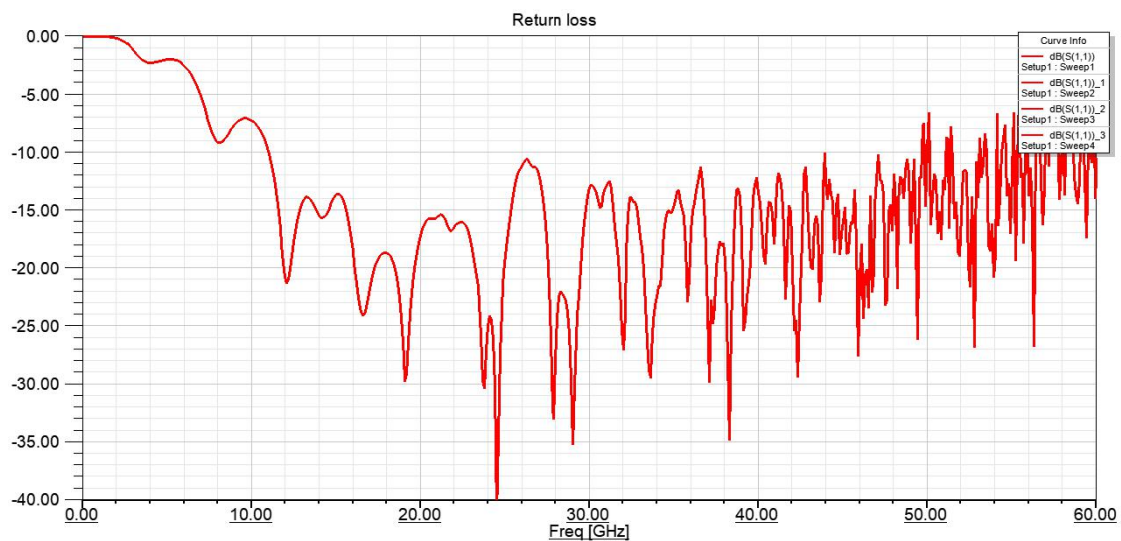


Fig. 13. The amplitude frequency characteristics with regard to the return loss of the antenna represented in Fig. 12.

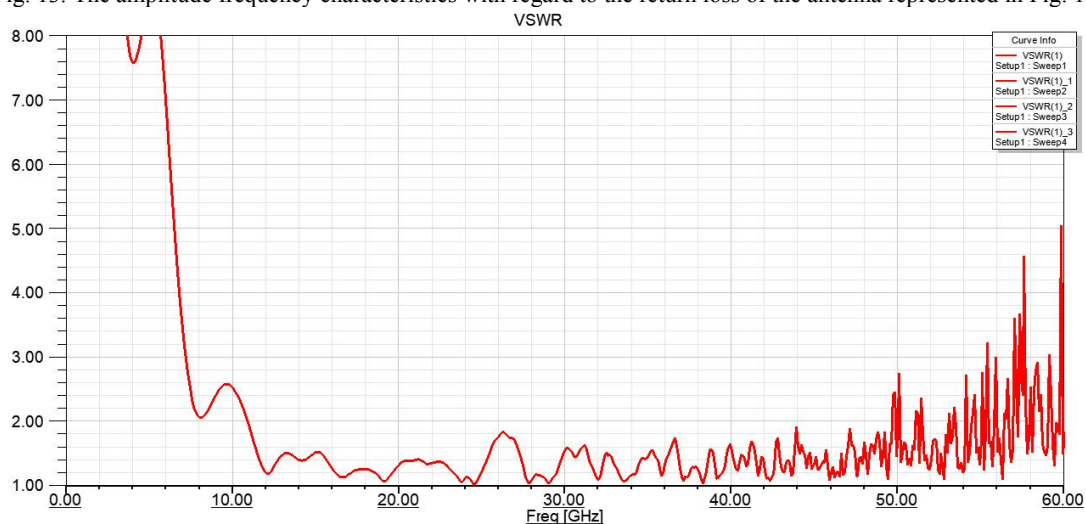


Fig. 14. The frequency Dependency of VSWR the antenna represented in Fig. 12.

Considering the obtained parameters, as well as more simple geometry, the antenna based on the “singular” ring had been chosen for the further scaling for the purpose of the decrease of the lower working limit. As a result, the super-broadband antenna had been developed with the external diameter of 3 inches (76.2 mm) based on the continuous singular ring, which is represented in Fig. 15–17. Its port is located in the gap between two strips. In terms of criterion $VSWR = 2$ the lower limit of the frequency range of the scaled antenna amounts to 3.653266 GHz. Regarding the upper limit of the working frequency area, the outlier can be considered in this regard, which arises at the frequency level of 38.6 GHz. As a result, the frequency selectivity band of the antenna in terms of $VSWR = 2$ amounts to $38.6 - 3.653266 = 34.9467$ GHz, and the frequency ratio is approximately $10.566 = 38.6 / 3.653266$. The calculation of the fractional bandwidth according to formula (11) results in:

$$(38.6 + 3.653266) / 2 = 21.126633 \text{ GHz}; 34.9467 / 21.126633 \approx 1.65415.$$

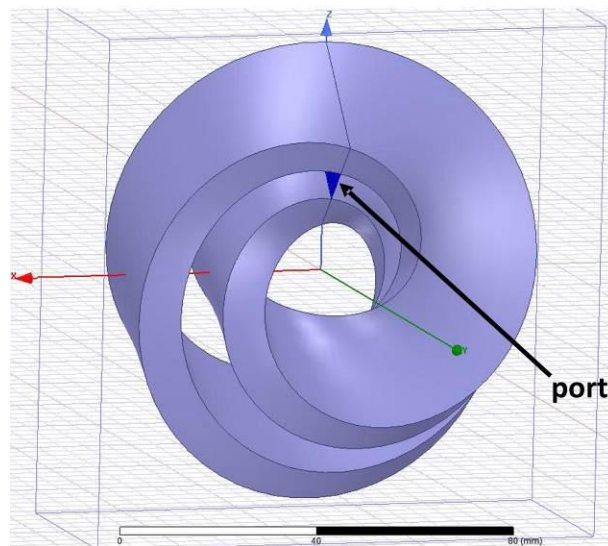


Fig. 15. The antenna configuration with the external diameter of 3 inches (76.2 mm).

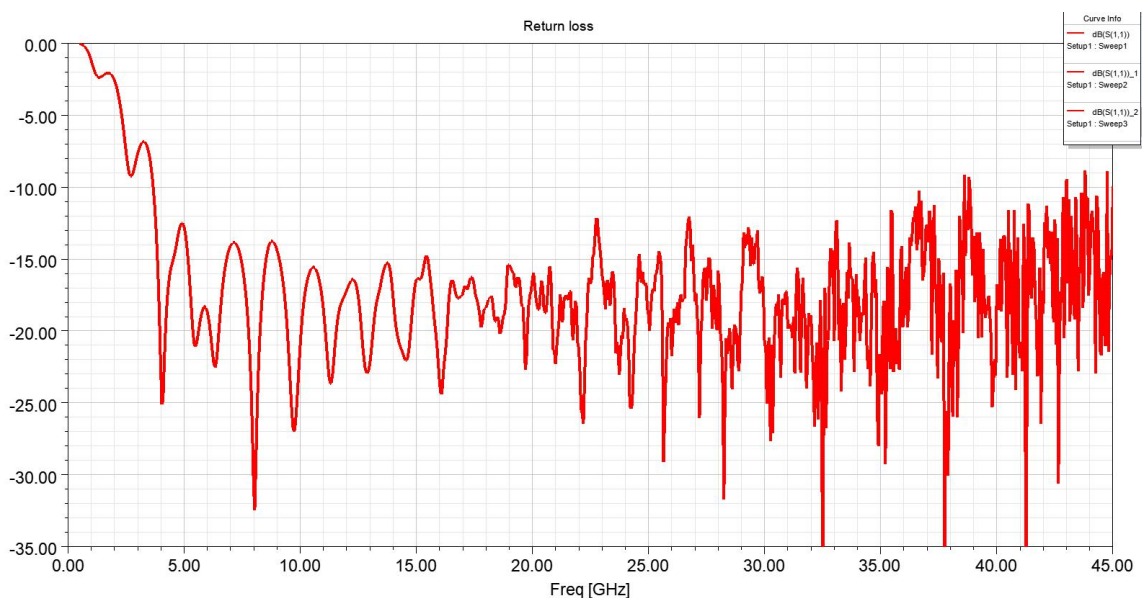


Fig. 16. The return loss of the antenna represented in Fig. 15.

The further increase of the external diameter of the antenna while preserving all the geometrical proportion, as expected, is accompanied by the shift of working frequency range down in terms of the frequency level, shrink in terms of its ultimate bandwidth and frequency ratio.

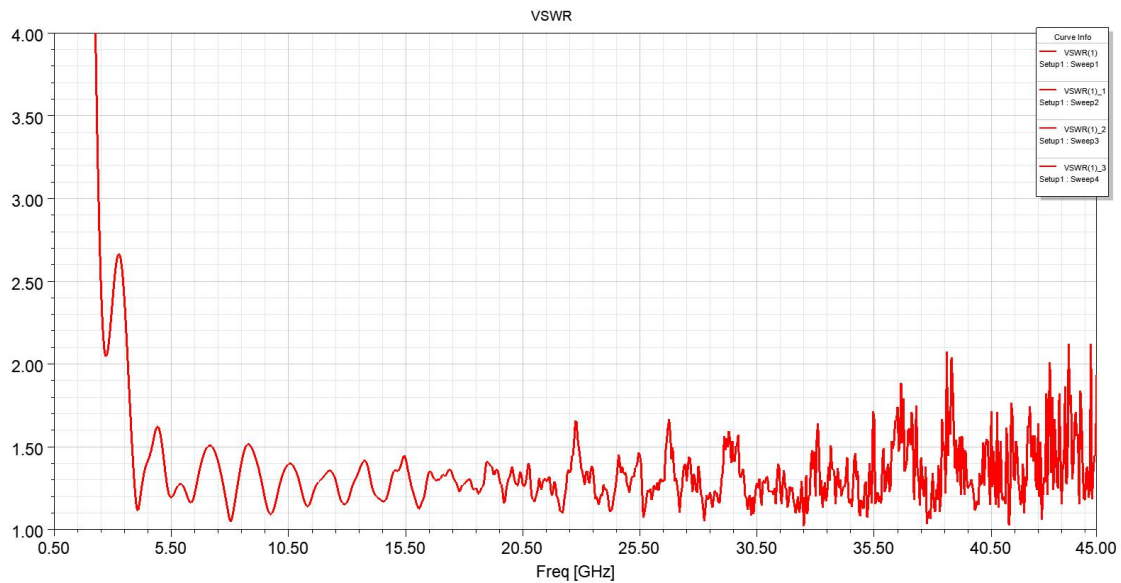


Fig. 17. VSWR of the “singular” antenna with the external diameter of 3 inches (76.2 mm).

For example, at the external diameter of 3.5 inches (88.9 mm), the lower frequency limit shifts to 3.15 GHz, and the upper one shifts to 26.250 GHz. Correspondingly, the overall frequency shrinks to 23.1 GHz and the frequency ratio amounts 8.33. As a result, the conclusion has been made that the best choice in this case is the diameter of 3.25 – 3.4 inches (88.55 – 86.36 mm), which allows the coverage of frequency ranges of cellular transmission 5G by means of only one antenna.

IV. ANTENNAS BASED ON CUT MOEBIUS STRIP

It is important to note that in the work [10] the execution of cut in the external ring of the double band antenna was applied as one of the potential directions for the extension of the working bandwidth. That is why, if we compare the results obtained for the reviewed antennas based on the Moebius rings with the data [10], then we can propose similar concept of the synthesis of the antenna structure based on the combination of the cut in the external surface and the power supply of the antenna by means of port located in the interstrip gap.

In order to verify this hypothesis, the antenna represented in Fig. 2.c. was taken as a basic point. At that, the cut was made in its external strip, representing the sector of 15 degrees (Fig. 18). Such modification, along with the constant external antenna radius of 1 inch (25.4 mm), enabled the obtainment of the response of approximately 9 GHz and shift of the lower limit of the broadband area from 20.7 GHz to 13.175 GHz (Fig. 19). At that, the upper boundary frequency, at which the condition $VSWR \leq 2$ is violated, has increased up to 63.51 GHz (Fig. 20). Therefore, the primary working frequency range of the ring antenna has extended to 50.35 GHz, and the frequency range was managed to be increased to 4.82. It should be noted that the similar calculation for the strip cut, representing the sector of 7 degrees, has led to less significant advantage.

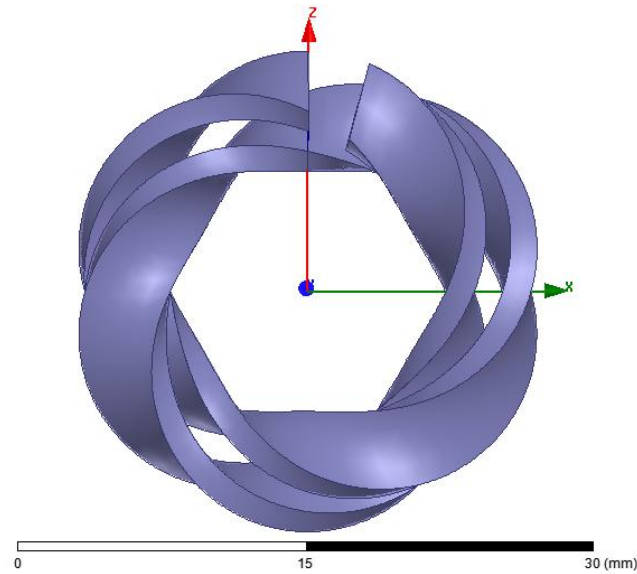


Fig. 18. The modification of the antenna represented in Fig. 1.c with the strip cut (Y-axis is directed away from the viewer).

In this regard, the obtained results have become the basis for the further search for the critical dimension of the strip cut, which will enable the obtainment of the maximum increase of the working frequency range of the antenna. For this purpose, the selective modelling of the antennas structures with the strip cuts being 30, 45 and 60 degrees has been performed. As expected, the cut of 45 degrees (Fig. 21) allowed the merge of the work area in the response region at the level of 9.2 GHz with the broadband area at the level exceeding 13 GHz (Fig. 22), hereinafter referred to in Fig. 19, 20. It took place due to the predictable decrease of the amplitude of the VSWR outlier, represented in Fig. 19, 20 at the level of 12 GHz to the value not exceeding 2. As a result, additional increase of the bandwidth of the working frequencies at the border of their minimum values has amounted 4 GHz (the working frequency range begins at the level of 9.1356 GHz).

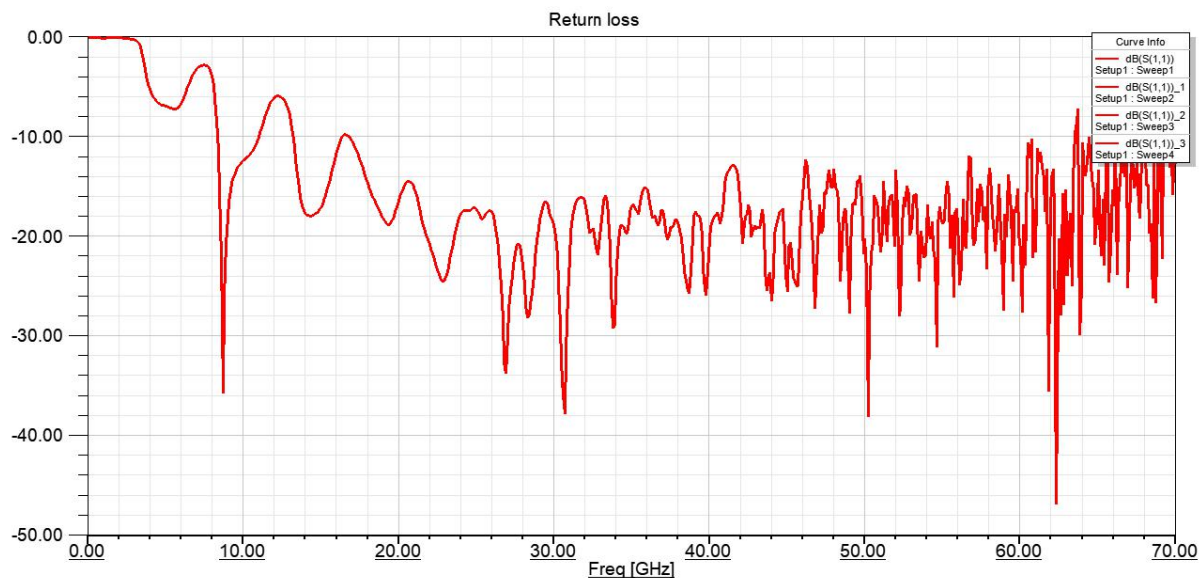


Fig. 19. The dependency of the return loss for the antenna represented in Fig. 18.

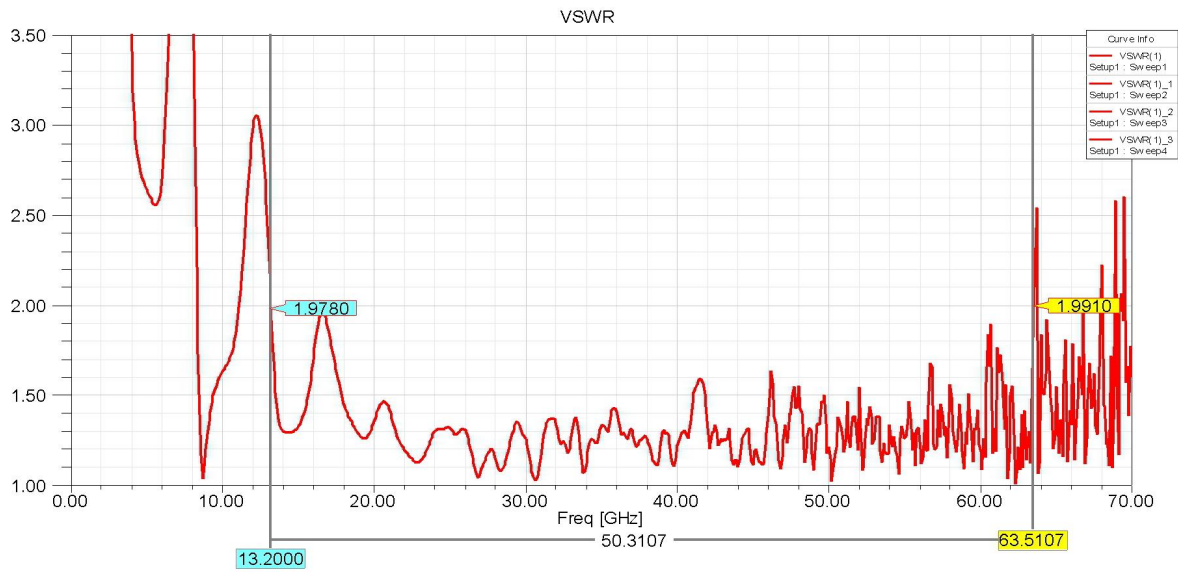


Fig. 20. The working bandwidth at VSWR=2 for the antenna represented in Fig. 18.

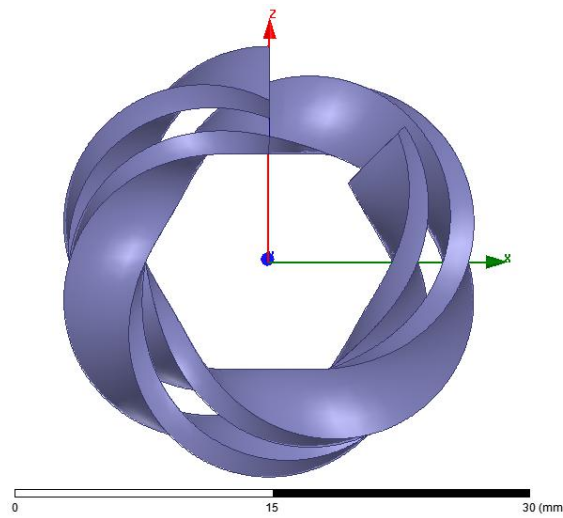


Fig. 21. Modification of the antenna represented in Fig. 18 with 45-degrees cut in the strip.

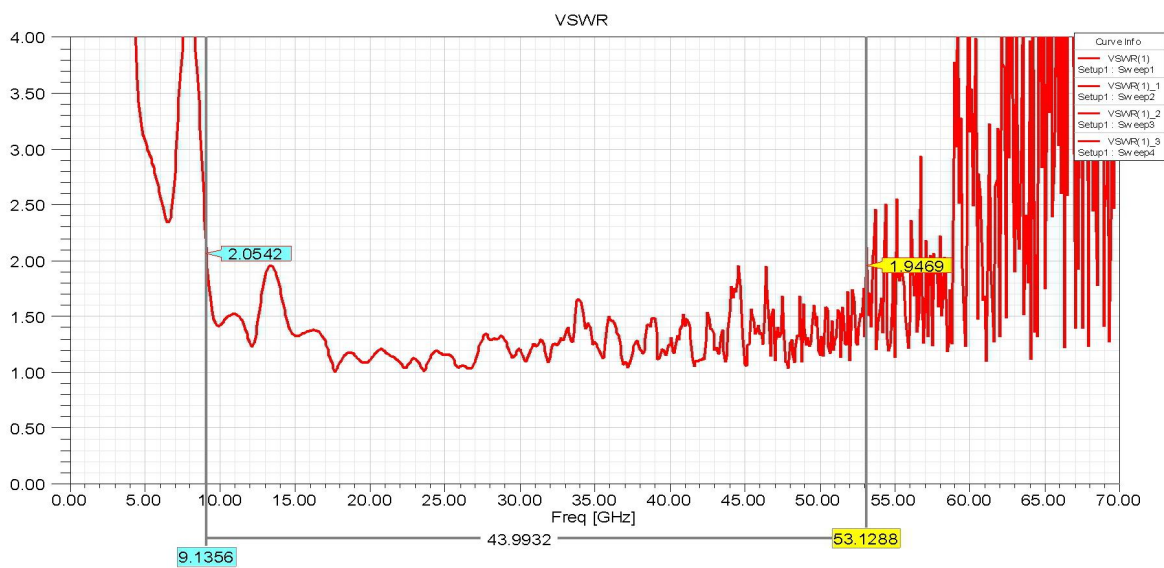


Fig. 22. Dependency of VSWR for the antenna represented in Fig. 21.

The further increase of the cut sector up to 60 degrees causes the extension of the lower level to the value of 9.4915 GHz. It indicates that the optimum point of the cut dimension is within sectors of 45 and 60 degrees, however its precise definition is out of scope of the present article.

The similar technique of modification of the antenna structure by means of the strip cut was applied for the singular ring as well. Such option with 45-degree sector of the cut is represented in Fig. 23.

In this case, based on Fig. 24, the lower limit of the frequency range had shifted to 8.3475 GHz, along with it the decrease of the upper limit down to the frequency of 46.3136 GHz took place. Regardless of the ultimate value of the bandwidth being reduced to 37.9661 GHz, its relative value, calculated by formula (11) increased up to 1.389, and the frequency ratio increased up to the value of 5.548. Therefore, the overall improvement of the frequency parameters of the antenna took place.

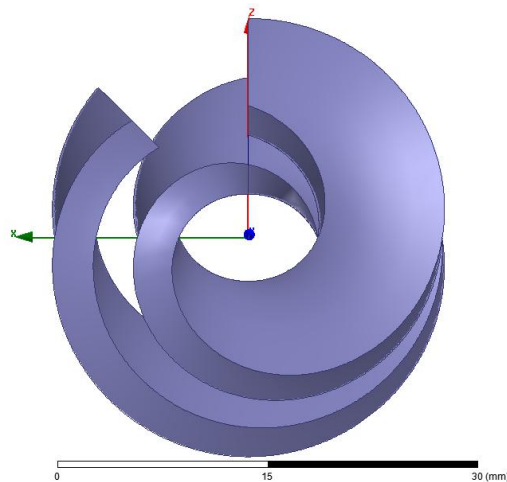


Fig. 23. Singular Moebius ring with the cut in 45-degree sector.

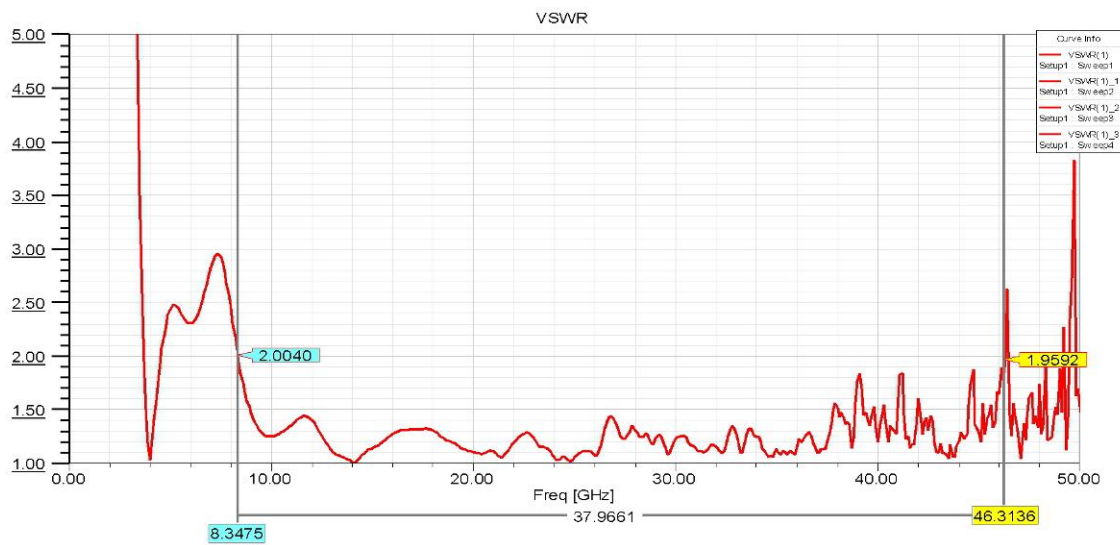


Fig. 24. Frequency Dependency of VSWR for 45-degrees cut.

In case the strip thickness is increased up to 3.5 mm with the interstrip gap of 3 mm. and the strip width of 9 mm. preserved unchanged, then the frequency ratio can be increased up to 6.52 considering the 45-degrees cut sector (Fig. 25). At that, the insignificant increase of the lower limit of the frequency range enabled its significant extension in terms of the upper frequencies level (up to

55.4746 GHz).

In case of the even further increase of the strip thickness, it has an opposite effect. For example, with the strip thickness of 4.5 mm, the chaotic outliers in the region of the upper limit of the working range took place due to the alignment discrepancies, which brings the frequency ratio down to 5.66 (Fig. 26). It should be also noted that the thickness of 4.5 mm considered in this case is the maximum possible strip thickness, because the further thickness increase becomes impossible without the short circuit following the strips adjoined.

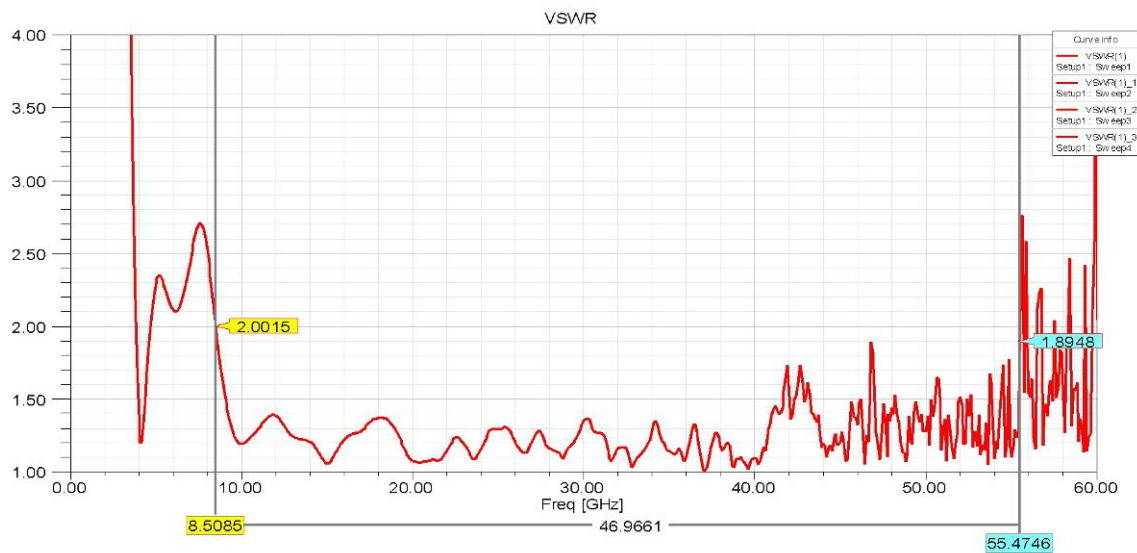


Fig. 25. VSWR of the singular ring (Fig. 22), where the strip thickness is increased up to 3.5 mm.

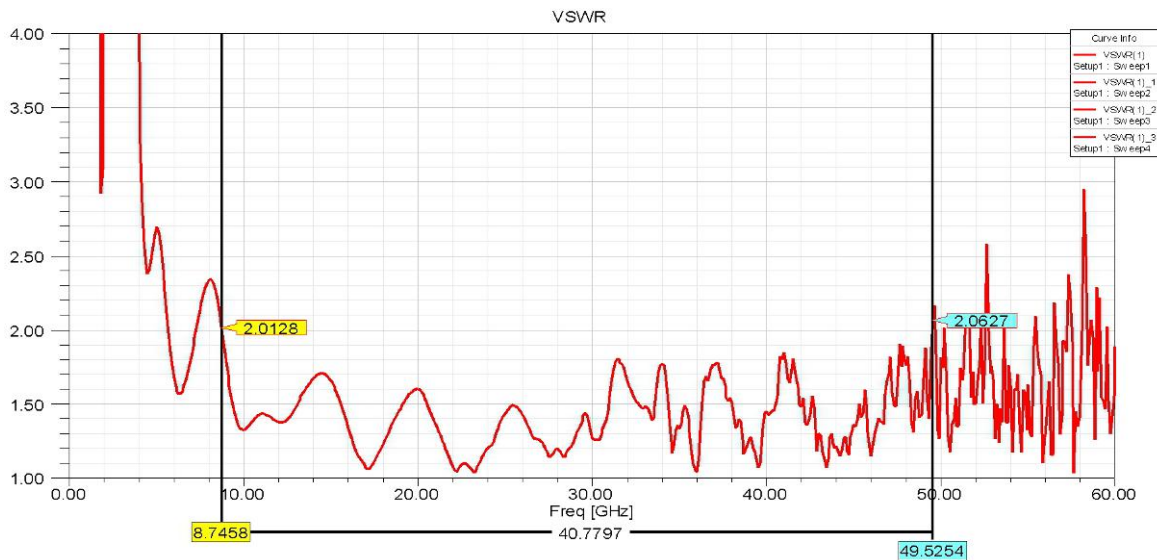


Fig. 26. VSWR of the singular ring, where the strip thickness is increased up to 4.5 mm with the interstrip gap of 3 mm, strip width of 9 mm, and 45-degree cut sector.

Due to the limited size of the article, it did not include radiation pattern estimates for all proposed antennas. However, paying tribute to tradition, as an example in fig. 27 shows 3D and 2D radiation patterns for an operating frequency of 25 GHz (which is within the bandwidth of the antenna represented in Fig. 6). In general, the form of the radiation pattern depends on the operating frequency underlying the solution and the environmental conditions around the antenna. It is important that the

radiation pattern of an individual element is not essential for antenna arrays. Moreover, it can be changed and customized, for example, using a metamaterial.

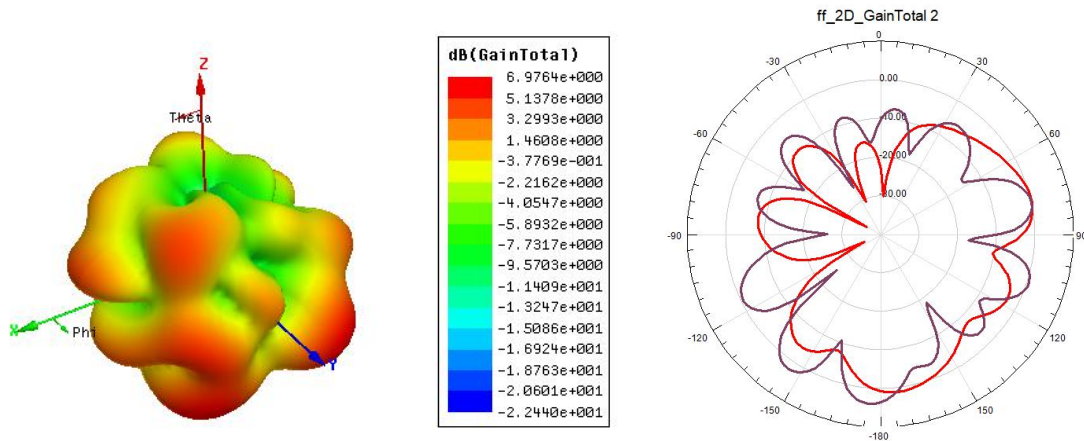


Fig. 27. The assessment of the radiation pattern of the antenna represented in Fig. 6 of the work (obtained in Ansys EM Suite 2021 R1).

The practical realization of proposed antennas is possible based on the technique of the additive manufacturing. The similar publications had been known for more than 7 years. At that the application of the specific software is reasonable, for example: Ansys Additive Manufacturing 3D Printing Simulation Software. The authors had tested several techniques of the manufacturing of the proposed antenna design. Particularly, there are results of 3D printing with the post-processing in Fig. 28. At that both conductive and dielectric materials had been used. In case when non-conductive materials are used, it is necessary to perform metallic coating of the surface, covering it with the conductive material using the electroforming method.

The alternative variant implies the application of 3D printing for the manufacturing of the cast molds for the subsequent casting of the antenna of the targeted design: 3D printing and lost polymer casting or castable wax resin from Formlabs Inc. (USA, Fig. 29). The specified approaches enable the focus on the various material options (including composites) or their combinations for the manufacturing of such antennas. Nevertheless, this research trend is out of frames of the present work.



Fig. 28. Antenna made of the conductive plastic using 3D printing method



Fig. 29. The antenna variant, manufactured by means of casting method.

On the other hand, the provision of the fastening and fixation of the proposed antenna elements within the constructions of the telecommunication and radiolocation equipment, including the development of the antenna arrays (for example, for the realization of MIMO or Massive-MIMO technologies) is possible based on the solutions which had been reviewed in patent [20]. Such constructions also provide the realization of the power supply system for the antenna. The examples of the corresponding technical solutions are represented in Fig. 30.

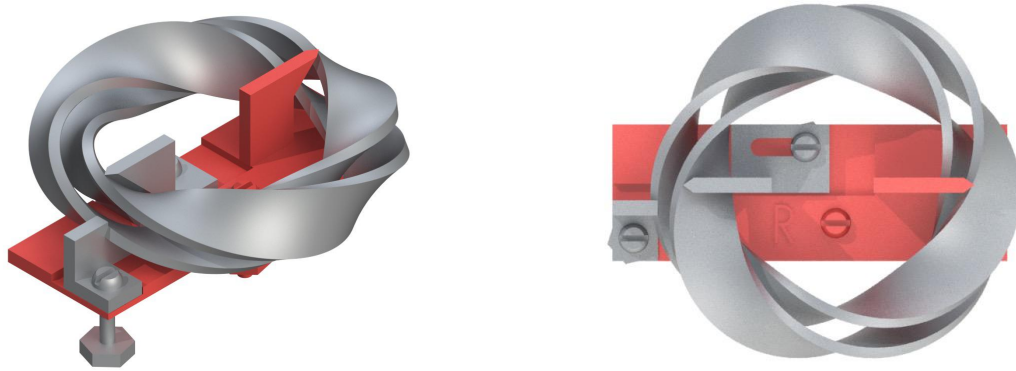


Fig. 30. The antenna fixation design [20].

V. CONCLUSION

Three possible options of the feeder port location for the active ring antenna had been reviewed in this article:

- with the cut in one of the strips, within which the signal port is placed;

- application of continuous Moebius ring, without any discontinuities, with the port located in the gap between the strips;

- with the cut in one of the strips and placement of the signal port into the interstrip gap.

The first of the indicated options appeared to be unacceptably narrowband, while the super-broadband antennas with the port placed between two strips represented the best results. In particular, the frequency independent antenna with the external diameter of 2 inches (50.8 mm) and based on the singular continuous Moebius ring has a bandwidth 38.648 GHz (from 11 to 49.648 GHz), and its frequency ratio (correlation of maximum operation frequency to the minimum one) exceeds 4.5. The corresponding bandwidth of the broadband antenna based on the ring with the star of David shape has amounted 32 GHz (from 14 to 46 GHz).

The execution of the cut in the strip enables the improvement of the antenna characteristics. By means of varying its angular size, it was established that its optimum value was within the range of 45 – 60 degrees. For example, for the antenna represented in Fig. 20 this 45-degrees cut made it possible to extend the lower limit of the working frequency range to 9.1356 GHz.

Along with the antennas, for the structure synthesis of which the triple and quintuple spin of the double Moebius strip had been applied, the worth one to be noted is the frequency independent antenna based on so called “singular” ring characterized by the single spin of the strip. The “singular”

structures of the antennas appeared to be the most broadband from among all the considered ones in term of their characteristics, and surpassed the antennas with the port located between the strips, having pentangular and hexagonal area in the center region, in terms of the obtained values. For the maximization of the frequency ratio of mentioned “singular” antenna, it is necessary to vary the strip thickness as well as the external diameter of its surface, enabled within the cylinder. The example of the effectiveness of such approach has become, e.g., the obtainment of the frequency ratio of more than 10.5 for the super-broadband antenna with the external diameter of 3 inches (76.2 mm) based on the continuous singular ring (Fig. 15). The further optimization of the structure is also possible based on the change of the cut size in the strip.

Actually, the synthesized antennas have a frequency band greater than the ultra-wideband antennas proposed in [21] and occupy the intermediate niche between the double strip ring antennas [7]–[10] and the printed antennas, described in [22], [23] in terms of their characteristics. It makes it possible to use them in integrated communication, radio location, radio monitoring and navigation, both as independent structural units and as parts of wheeled gear structures (wheel antennas [8] of the land crewless platforms as well as cycloplanes).

The further research of the antenna structures proposed in this article should be concentrated on the search for the optimum balance of their geometrical parameters with regard to the specific technical tasks. Moreover, the solution of the problem of the broadband power supply of the antenna, e.g., by means of the merge of various working frequency ranges and corresponding alignment of the power supply port, has been left beyond the scope of this article. At that, the multirange fractal structures, which can be used for the excitation of the considered antennas types simultaneously in several chosen ranges within the entire working frequency range, are worth noticing as well.

REFERENCES

- [1] J. Huang, Z. Fei, T. Wang, X. Wang, F. Liu, H. Zhou, J. A. Zhang and G. Wei, “V2X-communication assisted interference minimization for automotive radars,” *China Communications*, vol. 16, pp.100–111, Oct. 2019. DOI: 10.23919/JCC.2019.10.007.
- [2] M. Bekar, C. J. Baker, E. G. Hoare and M. Gashinova, “Joint MIMO Radar and Communication System Using a PSK-LFM Waveform with TDM and CDM Approaches,” *IEEE Sensors Journal*, vol. 21, No. 5, pp. 6115–6124, March 2021. DOI: 10.1109/JSEN.2020.3043085.
- [3] A. Zinchenko, V. Slyusar, N. Korolyuk and E. Korshets, “The Method of Open Space Selection of Signals for Radcom Systems,” in *Proc. 3rd Int. Conf. on Advanced Information and Communications Technologies*, Lviv, Ukraine, pp. 404–408. DOI: 10.1109/AIACT.2019.8847826.
- [4] G. Duggal, S. Vishwakarma, K. V. Mishra and S. S. Ram, “Doppler-Resilient 802.11ad-Based Ultra-Short Range Automotive Joint Radar-Communications System,” *IEEE Transactions on Aerospace and Electronic Systems*, vol. 56, Issue 5, pp. 4035–448, May 2020. DOI: 10.1109/TAES.2020.2990393.
- [5] K. V. Mishra, M. R. Bhavani Shankar, V. Koivunen, B. Ottersten and S. A. Vorobyov, “Toward Millimeter-Wave Joint Radar Communications: A Signal Processing Perspective,” *IEEE Signal Processing Magazine*, vol. 36, Issue 5, pp. 100–114, Sept. 2019. DOI:10.1109/MSP.2019.2913173.
- [6] M. Kiviranta, I. Moilanen and J. Roivainen, “5G Radar: Scenarios, Numerology and Simulations,” in *2019 Proc. Int. Conf. on Military Communications and Information Systems*, Budva, Montenegro. DOI: 10.1109/ICMCIS.2019.8842780.
- [7] I. Sliusar, V. Slyusar, S. Voloshko, A. Zinchenko and Y. Utkin, “Synthesis of a Broadband Ring Antenna of a Two-Tape Design,” in *Proc. 12th Int. Conf. on Antenna Theory and Techniques*, Kharkiv, Ukraine, 2020, pp. 161–165. DOI: 10.1109/UkrMW49653.2020.9252793.
- [8] V. Slyusar, I. Sliusar and V. Shut, “The wheel antennas MIMO for rovers,” in *Proc. V Int. research and training conf. Study of modern problems of civilization, Oslo, Norway, 2020*, pp. 471–478. DOI: 10.46299/ISG.2020.II.V.

- [9] I. Sliusar, V. Slyusar, S. Voloshko, A. Zinchenko and L. Degtyareva, "Synthesis of quasi-fractal ring antennas," in *Proc. 6th Int. Scientific-Practical Conf. Problems of Infocommunications. Science and Technology*, Kyiv, Ukraine, 2019, pp. 741–744. DOI: 10.1109/PICST47496.2019.9061286.
- [10] I. Sliusar, V. Slyusar, S. Zub and D. Teleshun, "Broadband antennas based on ring geometry," *Control, Navigation and Communication Systems. Academic Journal*, vol. 2, pp. 173–179, May 2020. DOI:10.26906/SUNZ.2020.2.173. (In Ukrainian).
- [11] T. J. Brown, "Mobius Capacitor", U.S. Patent 4 599 586, July 8, 1986.
- [12] A. K. Poddar and U. L. Rohde, "Metamaterial Möbius Strips (MMS): Application in Resonators for Oscillators and Synthesizers," in *2014 Proc. IEEE Int. Frequency Control Symp.* DOI:10.1109/fcs.2014.6859924.
- [13] A. Poddar, U. Rohde and T. Itoh, "Metamaterial Möbius Strips (MMS): Tunable Oscillator Circuits," in *2014 Proc. IEEE MTT-S Int. Microwave Symp. Tampa, USA*, pp. 1–4.
- [14] Clifford A. Pickover. *The Mobius strip. Dr. August Mobius's Marvelous Band in Mathematics, Games, Literature, Art, Technology, and Cosmology*. Published by Thunder's Mouth Press. – 2006. – Pp. 64–65.
- [15] Manfredo P. do Carmo. *Differential Geometry of Curves and Surfaces*. Prentice-Hall Inc., Englewood Cliffs, New Jersey. – 1976. – Pp. 106–107.
- [16] Sebastian Montiel, Antonio Ros, *Curves and surfaces*, American Mathematical Society, Second Edition. – 2009. – Pp. 71–74.
- [17] Alfred Gray. *Modern Differential Geometry of Curves and Surfaces with Mathematica^R*. Third Edition by Elsa Abbena and Simon Salamon, Chapman and Hall/CRC, 2006. – Pp. 339–340.
- [18] PTC Mathcad Online Store: Mathcad Free Trial. Available: <https://www.mathcad-store.co.uk/mathcad-free-trial>.
- [19] *Assessment of Ultra-Wideband (UWB) Technology*, OSD/DARPA Ultra-Wideband Radar Review Panel, Battelle Tactical Technology Center, Contract No. DAAH01-88-C-0131, ARPA Order 6049, July 13, 1990.
- [20] Sergey Sheleg, Vadym Slyusar, Ihor Sliusar, "Double-negative metamaterial unit cell", US Design Patent US D937777 S, December 7, 2021.
- [21] I. Aggarwal, S. Pandey and M. R. Tripathy, "A High Gain Super Wideband Metamaterial Based Antenna," *Journal of Microwaves, Optoelectronics and Electromagnetic Applications*, vol. 20, No. 2, pp. 248–273, June 2021. DOI: 10.1590/2179-10742021v20i21147.
- [22] R. A. Santos and S. Jr. Arismar Cerqueira, "A low-profile and ultra-wideband printed antenna with a 176% bandwidth," *Journal of Microwaves, Optoelectronics and Electromagnetic Applications*, vol. 16, No. 1, pp. 59–69, March 2016. DOI: 10.1590/2179-10742017v16i1621.
- [23] N. K. Darimireddy, R. R. Reddy, and A. M. Prasad, "A Miniaturized Hexagonal-Triangular Fractal Antenna for Wide-Band Applications," *IEEE Antennas and Propagation Magazine*, pp. 104–110, April 2018. DOI:10.1109/MAP.2018.2796441.